Polyoxometalates

DOI: 10.1002/ange((will be filled in by the editorial staff))

Aiding the Self-Assembly of Supramolecular Polyoxometalates under Hydrothermal Conditions to Precursors of Complex Functional Oxides**

*Maricruz Sanchez Sanchez, Frank Girgsdies, Mateusz Jastak, Pierre Kube, Robert Schlögl, and Annette Trunschke**

((Dedication----optional))

The activation of small alkane molecules originating from natural gas or renewable resources will offer alternative pathways to functionalized hydrocarbons in a post-petroleum era. Crystalline or nano-crystalline molybdenum-vanadium based multi-metal oxides have been identified as versatile heterogeneous catalysts for selective oxidation of ethane,[1] propane,[2] and propene.[3]

The crystal structures of these oxides show common structural attributes. In the framework of the tetragonal M_5O_{14}-type (M= Mo, V, W, Ti, Nb) structure (ICSD 27202),[4] and in the orthorhombic M1 structure (ICSD 55097) of MoVTe(Sb)Nb(Ta) oxides,[5] metal-oxide polyhedra are cross-linked in the crystallographic *ab* plane by sharing corners or edges as shown in Schema 1. Needle-like nano-crystals growth along the crystallographic *c* axis by linking corners of the polyhedra resulting in a short lattice constant *c* at 0.4 nm and formation of channels with different sizes typical for oxidic bronzes. The structural motif $\{(M)M_5\}$, (M= Mo,V,Nb), which is composed of a pentagonal bipyramidal MO_7 unit that shares the five edges of the planar pentagon with five MO_6 octahedra (Schema 1), is another common feature that is also known as a key constituent of larger structural aggregates appearing in the rich and beautiful chemistry of reduced molybdates in solutions.[6] Icosahedral molecular systems of the type $\{(Mo^{VI})Mo_5^{VI}\}_{12}(linker)_{30}$, called Keplerates, have been considered as donor of the $\{(M)M_5\}$ building blocks in the M_5O_{14} synthesis[7] and the hydrothermal synthesis of Mo_3VO_x, MoVSb and MoVTeNb mixed oxides with M1 structure.[8]

The complexity of the M1 structure provides site isolation, as it is required for a high selectivity in oxidation reactions of C3 and C2 feedstock.[9] Current synthetic approaches to phase-pure M1 suffer from insufficient reproducibility,[10] and apparently similar M1 catalysts may feature very different catalytic behaviour.[9, 11] Controlled synthesis of M1 with predictable surface properties requires deeper understanding of the inorganic reactions proceeding during assembly of structural building blocks and crystallization.

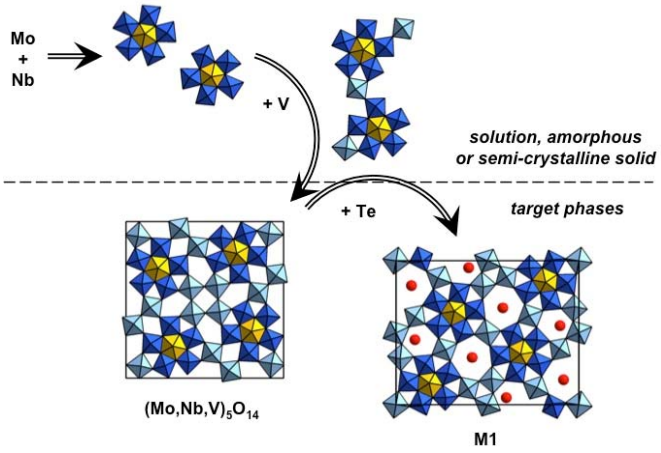

Scheme 1. Representation of the assembly of structural motives during formation of the target phases M1 and $(Mo,Nb,V)_5O_{14}$.

In this work, we have studied the formation of mixed MoVTeNb oxides under hydrothermal conditions by *in-situ* Raman spectroscopy. The spectroscopic information enabled the design of a new, accelerated and reproducible hydrothermal route towards precursors of phase-pure M1. Modular cross-linking of structural building blocks as outlined in Scheme 1 directs the synthesis towards the desired product avoiding the co-formation of unwanted phases.

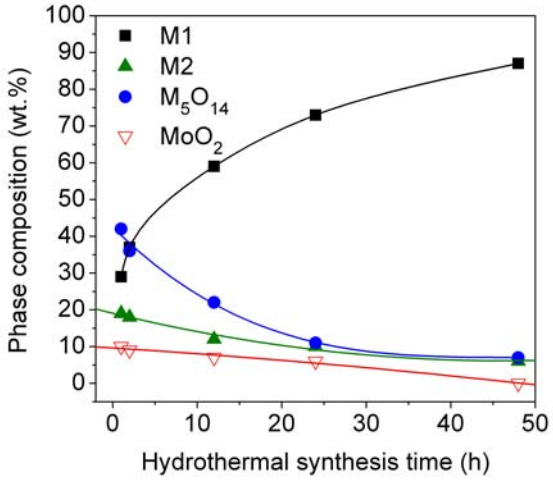

Figure 1. Evolution of phase composition of MoVTeNb oxides as a function of the hydrothermal reaction time at T=448 K, p=14 bar.

In conventional hydrothermal recipes, the synthesis of MoVTeNb oxides is performed starting from suspensions of the

[*] Dr. M. Sanchez-Sanchez, Dr. F. Girgsdies, M. Jastak, P. Kube, Prof. Dr. R. Schlögl, Dr. A. Trunschke
Department of Inorganic Chemistry
Fritz-Haber-Institut der Max-Planck-Gesellschaft
Faradayweg 4-6
Fax: (+49) 30 8413 4405
E-mail: trunschke@fhi-berlin.mpg.de
Homepage: http://www.fhi-berlin.mpg.de/acnew/welcome.epl.

[**] This work was supported by the German Research Foundation through the cooperate research center "Structure, dynamics, and reactivity of transition metal oxide aggregates" (Sonderforschungsbereich 546, http://www.chemie.hu-berlin.de/sfb546). We thank the Max Plack Institute for Bioinorganic Chemistry, Mühlheim, for providing the Raman spectrometer. The authors thank Dr. Tom Cotter for his help with data analysis, Gisela Lorenz for N_2 physisorption measurements, and Achim Klein-Hoffmann for chemical analysis by X-ray fluorescence. The authors thank the referees for the profound discussion.

Supporting information for this article is available on the WWW under http://www.angewandte.org or from the

oxides or metal salts in water and keeping the mixture for 48 h at T=448 K under autogeneous pressure (Fig. S1A).[2, 8d] Fig. 1 shows the phase composition of hydrothermal reaction products after crystallization as a function of time. The chemical composition of complementary precipitates and mother liquors are presented in Figure S2 of the Supporting Information. Hydrothermal synthesis for short times yielded a mixture of M_5O_{14}-like oxide (M= Mo, V, Nb), the pseudo-hexagonal M2 phase (ICSD 55098)[5b], the M1 phase, and a rutile-like phase MO_2 (M=Mo,V). With increasing reaction times, the fractions of M_5O_{14} and M2 decrease while M1 becomes the main product.

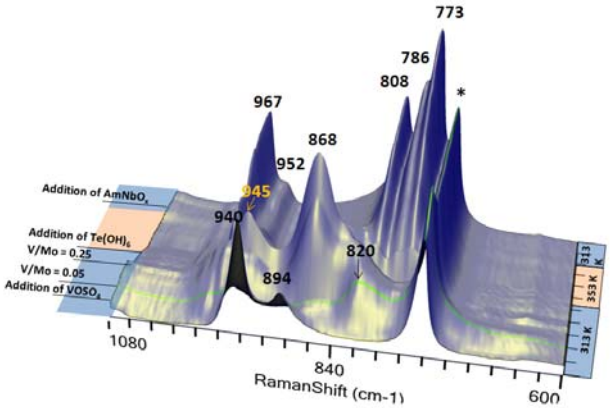

Figure 2. *In-situ* Raman spectra during preparation of the aqueous suspension before hydrothermal synthesis. For details see Supporting Information. Symbol (*) indicates a band of the sapphire window of the Raman probe.

The synthesis was monitored applying *in-situ* Raman spectroscopy. The assignment of the bands is discussed in detail in the Supporting Information. Mixing Mo and V salts at 313 K (Fig. 2) results in the formation of $\{Mo_{72}V_{30}\}$ Keplerate ions (868, 945 cm^{-1})[12] as soon as the acidification of the solution by addition of vanadyl sulfate results in pH<4 (Fig. S3). This observation is in perfect agreement with the recently reported spontaneous formation of $\{(Mo)Mo_5\}_{12}\{Mo_2\}_{30}$-type Keplerates by addition of preformed $\{Mo^{V}O\}^{2+}$ units to an acidified molybdate solution.[13] These species contain the desired $\{(M)M_5\}$ structural motives that represent essential building blocks of the M1 structure, and V atoms are already situated in proper linking positions between these pentagonal units. The broad appearance between 1000 and 940 cm^{-1} indicate the additional contribution of macroisopolyanions $[Mo_{36}O_{112}]^{8-}$ (Fig. S3).[14] Subsequent addition of Te and heating to 353 K causes re-dissolution of the pre-formed $\{Mo_{72}V_{30}\}$ Keplerate clusters and formation of heteropolymolybdate anions $[(TeO_3)_2Mo_{12}O_{36}]^{4-}$ (773, 786, 808, 967 cm^{-1}),[15] which are structurally closer related to the M2 phase and to other undesired crystalline phases like $TeMo_5O_{16}$. Free telluric acid (644 cm^{-1}),[16] Anderson-type heteropolyanions $[Te(Mo,V)_6O_{24}]^{n-}$ (952, 1010 cm^{-1}),[17] and re-dissolved vanadium species (975, 1050 cm^{-1}) are also present. The final addition of $NH_4[NbO(C_2O_4)_2]\cdot xH_2O$ to the Mo-V-Te solution after cooling to 313 K did not change the Raman spectrum.

During subsequent heating from 313 K to hydrothermal reaction temperature 448 K (Fig. 3), molybdotellurates are decomposed at T>393 K under intermediate formation of $[Mo_{36}O_{112}]^{8-}$ ions (988, 952 and 912 cm^{-1}) leading to precipitation of nano-crystalline M_5O_{14} (M=Mo,V,Nb) oxide (835, 930 cm^{-1}) at T > 418 K,[18] which is in good agreement with the predominance of this phase in the product obtained after short reaction times (Fig. 1). Since Nb is almost completely incorporated into the solid (Fig. S2), it is assumed that this element plays an important role in the formation of the M_5O_{14} phase owing to its preference to occupy the MO_7 pentagonal bipyramidal position in the $\{(M_5)M\}$ units.[5b]
The spectral changes under isothermal conditions (Fig. S4) become more evident by analyzing the covariance of the observed Raman bands (Fig. 4). The broad contribution between 900 and 800 cm^{-1}, which may indicate $\{(M)M_5\}$ units in nano-crystals of M_5O_{14} and M1 (Figs. S6-7),[7b] and the band at 952 cm^{-1} for $[Mo_{36}O_{112}]^{8-}$ anions in solution, remained almost unchanged during the entire reaction. The macro-isopolyanions can be considered as species existing in equilibrium with the solid phase, being responsible for the substantial amount of Mo detected in solution after synthesis. The main changes are related to the growth of bands at 969, 931, 880, 800, 726, and 323 cm^{-1}. Since the resulting product is the precursor of a mixture of M1, M2, M_5O_{14} and MO_2 phases (Fig. 1), an unambiguous assignment of these bands is not possible.

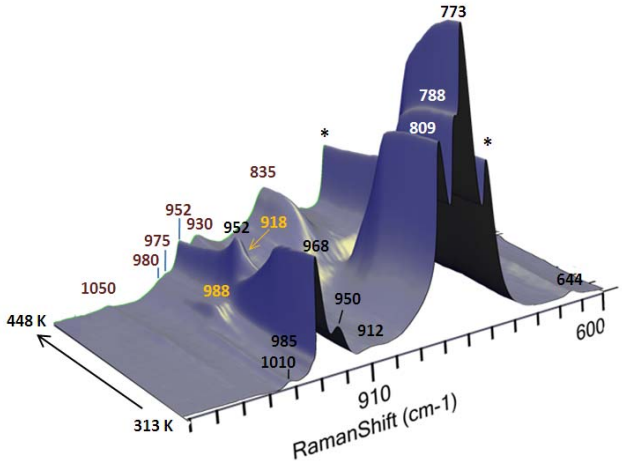

Figure 3. Raman spectra taken during heating from 313 K to 448 K.

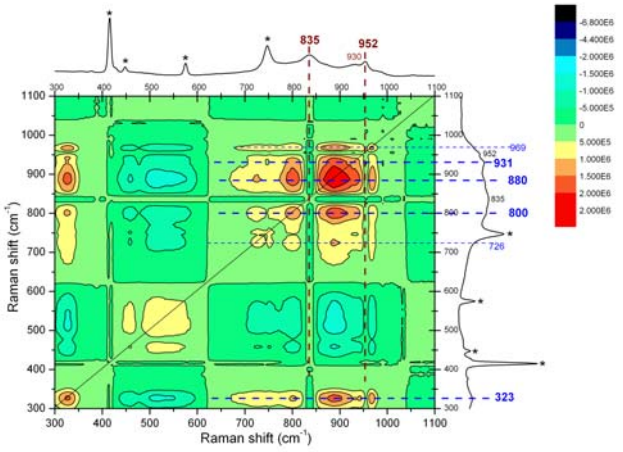

Figure 4. Covariance analysis of *in-situ* Raman bands measured during hydrothermal reaction at 448 K. Initial spectrum shown on top; spectrum after 15h on the right side.

Based on our knowledge acquired by *in-situ* Raman spectroscopy, we conceptually designed a novel, rational synthesis of phase-pure M1 MoVTeNb oxide by stepwise addition of V and Te under pressure (Fig. S1B). At first, a nano-crystalline oxide containing $\{(M)M_5\}$ units (812 cm^{-1}) was formed by hydrothermal reaction of Mo and Nb precursors at 448 K (Fig. S5). At this point, an aqueous solution of $VOSO_4$ is pumped into the autoclave with the aim to cross-link the pentagonal units with vanadium species, as depicted in Scheme 1. The subsequent introduction of Te as inorganic template is responsible for formation of nano-crystalline M1 (816, 870(sh), 919 and 975 cm^{-1}) with enhanced precursor yield (Tab. S1), which is of advantage in view of an improved control with respect to the final chemical composition of the solid. The isolated precipitate can be crystallized at 923 K in argon atmosphere resulting in phase-pure M1 (Figs. S6-7). The surface area of the new M1 is increased as a consequence of controlled initial precipitation of Mo species,

which takes place through the decomposition of Mo oxalates (bands at 904 and 951 cm^{-1} in Fig S5). The retarded addition of Te avoids the formation of Te-Mo polyanions in solution, allowing precipitation of higher amount of product in shorter synthesis times at lower temperatures. The new M1 catalyst is characterized by distinguished selectivity to acrylic acid in selective oxidation of propane resulting in an increase in space time yield by a factor of five (Tab. S1).

In summary, it is shown that the simultaneous study of multiple variables during formation of complex nano-structured solids in terms of inorganic systems chemistry[19] offers a great potential in directing the properties of materials towards desired functionalities.

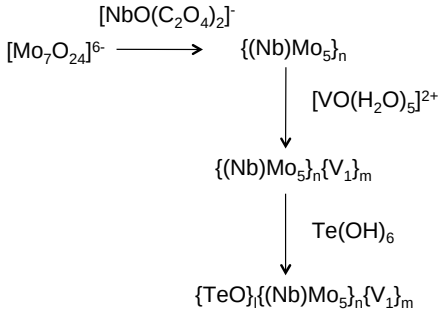

Schema 2. Step-wise synthesis of phase-pure M1 precursors.

In-situ investigation of nano-particle synthesis provides insight into molecular processes of self-assembly and precursor formation.[8a, 8c, 20] Many studies reported so far are focussed on binary and ternary systems.[20c] However, the complexity of materials required in the field of heterogeneous catalysis necessitates controlled synthesis strategies to create multi-component systems involving structures in the nano- and micro-meter length scale creating surface terminations unexpected from the bulk crystal structure.[21] The present study of a practical system with substantial chemical complexity exemplifies a new paradigm of inorganic synthetic chemistry. Complex functional materials are assembled by generating sequences of reactions creating each a sub-unit of the target structure. This was enabled by combining the mild reaction environment of solvothermal synthesis with novel analytical capabilities that guide through *in-situ* monitoring of identified intermediates. It allows handling a wide spectrum of chemical elements. We describe here a platform procedure for a systemic synthesis approach aiming at generating complex functionality from structural inorganic concepts using a minimum of unit operations.

Experimental Section

The classical and step-wise synthesis procedures of MoVTeNb oxides are described in detail in the Supporting Information. *In-situ* Raman measurements were performed applying a Kaiser Optics Raman Spectrometer RXN1 equipped with a fiber-optic probe head, using a Laser wavelength of 785 nm. Experimental details of characterization techniques and catalytic tests are summarized in the Supporting Information.

Received: ((will be filled in by the editorial staff))
Published online on ((will be filled in by the editorial staff))

Keywords: hydrothermal synthesis · MoVTeNb oxides · M1 phase · *in-situ* · catalysis

[1] E. M. Thorsteinson, T. P. Wilson, F. G. Young, P. H. Kasai, *Journal of Catalysis* **1978**, *52*, 116.
[2] D. Vitry, Y. Morikawa, J. L. Dubois, W. Ueda, *Topics in Catalysis* **2003**, *23*, 47.
[3] J. B. Wagner, D. S. Su, S. A. Schunk, H. Hibst, J. Petzoldt, R. Schoegl, *Journal of Catalysis* **2004**, *224*, 28.
[4] L. Kihlborg, *Acta Chem. Scand.* **1969**, *23*, 1834.
[5] a)X. Li, D. Buttrey, D. Blom, T. Vogt, *Topics in Catalysis* **2011**, *54*, 614; b)P. DeSanto, Jr., D. J. Buttrey, R. K. Grasselli, C. G. Lugmair, A. F. Volpe, Jr., B. H. Toby, T. Vogt, *Zeitschrift fuer Kristallographie* **2004**, *219*, 152.
[6] a)A. Müller, C. Serain, *Accounts of Chemical Research* **2000**, *33*, 2; b)A. Müller, S. Polarz, S. K. Das, E. Krickemeyer, H. Bögge, M. Schmidtmann, B. Hauptfleisch, *Angewandte Chemie International Edition* **1999**, *38*, 3241; c)A. Müller, P. Kögerler, A. W. M. Dress, *Coordination Chemistry Reviews* **2001**, *222*, 193; d)A. Müller, P. Kogerler, C. Kuhlmann, *Chemical Communications* **1999**, 1347; e)A. Müller, S. Roy, *European Journal of Inorganic Chemistry* **2005**, *2005*, 3561.
[7] a)S. Knobl, G. A. Zenkovets, G. N. Kryukova, R. I. Maksimovskaya, T. V. Larina, N. T. Vasenin, V. F. Anufrienko, D. Niemeyer, R. Schlögl, *Physical Chemistry Chemical Physics* **2003**, *5*, 5343; b)S. Knobl, G. A. Zenkovets, G. N. Kryukova, O. Ovsitser, D. Niemeyer, R. Schlögl, G. Mestl, *Journal of Catalysis* **2003**, *215*, 177.
[8] a)M. Sadakane, N. Watanabe, T. Katou, Y. Nodasaka, W. Ueda, *Angewandte Chemie, International Edition* **2007**, *46*, 1493; b)M. Sadakane, K. Yamagata, K. Kodato, K. Endo, K. Toriumi, Y. Ozawa, T. Ozeki, T. Nagai, Y. Matsui, N. Sakaguchi, W. D. Pyrz, D. J. Buttrey, D. A. Blom, T. Vogt, W. Ueda, *Angewandte Chemie International Edition* **2009**, *48*, 3782; c)R. Canioni, C. Marchal-Roch, N. Leclerc-Laronze, M. Haouas, F. Taulelle, J. Marrot, S. Paul, C. Lamonier, J.-F. Paul, S. Loridant, J.-M. M. Millet, E. Cadot, *Chemical Communications* **2011**, *47*, 6413; d)A. Celaya Sanfiz, T. W. Hansen, F. Girgsdies, O. Timpe, E. Rödel, T. Ressler, A. Trunschke, R. Schlögl, *Topics in Catalysis* **2008**, *50*, 19.
[9] A. Celaya Sanfiz, T. W. Hansen, D. Teschner, P. Schnörch, F. Girgsdies, A. Trunschke, R. Schlögl, M. H. Looi, S. B. A. Hamid, *The Journal of Physical Chemistry C* **2010**, *114*, 1912.
[10] A. Trunschke, in *Nanostructured Catalysts: Selective Oxidation Reactions*, 1 ed. (Eds.: C. Hess, R. Schlögl), RSC Nanoscience & Nanotechnology, Cambridge, **2011**, pp. 56.
[11] Y. V. Kolen'ko, W. Zhang, R. N. d'Alnoncourt, F. Girgsdies, T. W. Hansen, T. Wolfram, R. Schlögl, A. Trunschke, *ChemCatChem* **2011**, *3*, 1597.
[12] A. Müller, A. M. Todea, J. van Slageren, M. Dressel, H. Bögge, M. Schmidtmann, M. Luban, L. Engelhardt, M. Rusu, *Angewandte Chemie International Edition* **2005**, *44*, 3857.
[13] C. Schäffer, A. M. Todea, P. Gouzerh, A. Müller, *Chemical Communications* **2012**, *48*.
[14] a)K.-H. Tytko, B. Schönfeld, B. Buss, O. Glemser, *Angewandte Chemie International Edition in English* **1973**, *12*, 330; b)A. Müller, E. Krickemeyer, S. Dillinger, H. Bögge, W. Plass, A. Proust, L. Dloczik, C. Menke, J. Meyer, R. Rohlfing, *Zeitschrift für anorganische und allgemeine Chemie* **1994**, *620*, 599.
[15] S. Himeno, K.-i. Sano, H. Niiya, Y. Yamazaki, T. Ueda, T. Hori, *Inorganica Chimica Acta* **1998**, *281*, 214.
[16] J. Gupta, *Nature* **1937**, *140*, 685.
[17] a)I. L. Botto, C. I. Cabello, H. J. Thomas, *Materials Chemistry and Physics* **1997**, *47*, 37; b)Y. Sun, J. Liu, E. Wang, *Inorganica Chimica Acta* **1986**, *117*, 23.
[18] G. Mestl, C. Linsmeier, R. Gottschall, M. Dieterle, J. Find, D. Herein, J. Jäger, Y. Uchida, R. Schlögl, *Journal of Molecular Catalysis A: Chemical* **2000**, *162*, 463.
[19] R. F. Ludlow, S. Otto, *Chemical Society Reviews* **2008**, *37*, 101.
[20] a)A. M. Beale, G. Sankar, *Chemistry of Materials* **2002**, *15*, 146; b)C. Kongmark, V. Martis, A. Rubbens, C. Pirovano, A. Lofberg, G. Sankar, E. Bordes-Richard, R.-N. Vannier, W. Van Beek, *Chemical Communications* **2009**, 4850; c)G. R. Patzke, Y. Zhou, R. Kontic, F. Conrad, *Angewandte Chemie International Edition* **2011**, *50*, 826; d)R. Kiebach, N. Pienack, W. Bensch, J.-D. Grunwaldt, A. Michailovski, A. Baiker, T. Fox, Y. Zhou, G. R. Patzke, *Chemistry of Materials* **2008**, *20*, 3022; e)R. I. Maksimovskaya, V. M. Bondareva, G. I. Aleshina, *European Journal of Inorganic Chemistry* **2008**, *2008*, 4906.
[21] W. Zhang, A. Trunschke, R. Schlögl, D. Su, *Angewandte Chemie International Edition* **2010**, *49*, 6084.

Entry for the Table of Contents (Please choose one layout)

Inorganic systems chemistry

Maricruz Sanchez Sanchez, Frank Girgsdies, Mateusz Jastak, Pierre Kube, Robert Schlögl, and Annette Trunschke*

_____ Page – Page

Guiding the Self-Assembly of Supramolecular Polyoxometalates under Hydrothermal Conditions to Precursors of Complex Functional Oxides

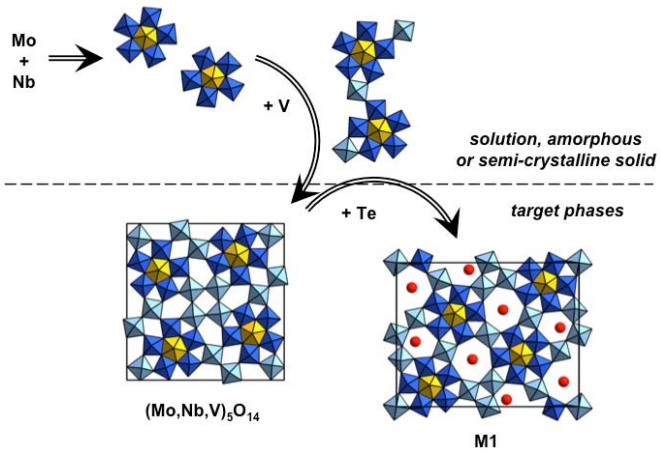

In-situ Raman spectroscopy allows insight into molecular processes under hydrothermal conditions during synthesis of technologically relevant, complex nano-structured MoVTeNb oxides. Based on the knowledge acquired with respect to the complicated cross-linked reaction network of polyoxometalate intermediates, an innovative synthesis procedure was developed that directs the synthesis more efficiently towards the desired product with improved functionality.

Supporting Information

Aiding the Self-Assembly of Supramolecular Polyoxometalates under Hydrothermal Conditions to Precursors of Complex Functional Oxides

Maricruz Sanchez Sanchez, Frank Girgsdies, Mateusz Jastak, Pierre Kube, Robert Schlögl, and Annette Trunschke

trunschke@fhi-berlin.mpg.de

Table of contents

1. Experimental Details

1.1. Classical hydrothermal synthesis of MoVTeNb oxides

MoVTeNb oxides were synthesized under hydrothermal conditions starting from a complex mixture with a Mo concentration of 0.26 mol/L that contains the metals in a molar ratio of Mo/V/Te/Nb = 1/0.25/0.23/0.12 by successive dissolution of 11.75 g (9.51 mmol) $(NH_4)_6Mo_7O_{24}$ (Merck, 81-83 % as MoO_3), 3.86 g (16.6 mmol) $VOSO_4 \cdot 5H_2O$ (Alfa Aesar, 99.9 %), 3.52 g (15.3 mmol) $Te(OH)_6$ (Fluka, > 99.0 %), and 3.80 g (7.94 mmol) $NH_4[NbO(C_2O_4)_2] \cdot 9.7H_2O$ (H.C. Starck 99.99 %) in 230 ml ultrapure water. The water was purified using the Milli-Q Synthesis System (MQ). At first, ammonium heptamolybdate was dissolved at 313 K in 200 mL H_2O, followed by addition of solid vanadyl sulfate. After 15 min stirring at 400 rpm, $Te(OH)_6$ was added in solid form and the suspension was heated up to 353 K and stirred for 20 min. Ammonium niobate (V) oxalate hydrate dissolved at 300 K in 30 mL water was added after cooling down the Mo-V-Te mixture to 313 K. In order to homogenize the Mo-V-Te-Nb synthesis gel, stirring was continued at 313 K for another 30 min. Then, the mixture was charged into an analytic autoclave HPM-PT-040 (400 mL) made of Hastelloy C22 (Premex Reactor GmbH). Hydrothermal synthesis was performed at T=448 K (heating ramp 5 K/min, cooling ramp 1.6 K/min) under autogeneous pressure of ca. 14 bar applying a stirring rate of 250 rpm. Catalyst precursor materials were prepared applying hydrothermal reaction times between 1 and 48 h. The temperature and pressure profiles of the 48 h experiment are shown exemplarily in Fig. S1A. Suspensions obtained after hydrothermal synthesis were separated by centrifugation at 3600 rpm for 10 min. The solid fractions were washed with 100 mL of H_2O and then centrifuged again at 3600 rpm for 30 min. Finally, washed solids were dried at 353 K for 16 h to obtain the precursor oxides. Thermal treatment of precursors was done in a rotary tube furnace (Xerion) under Ar flow (100 ml/min) at 923 K (heating rate 15 K/min) for 2 h.

Phase-pure M1 (internal sample number 11811) was obtained by applying the synthesis described above at 463 K for 12 hours (autogeneous pressure of ca. 17 bar). The precursor yield was 42 wt.% (6.2 g).

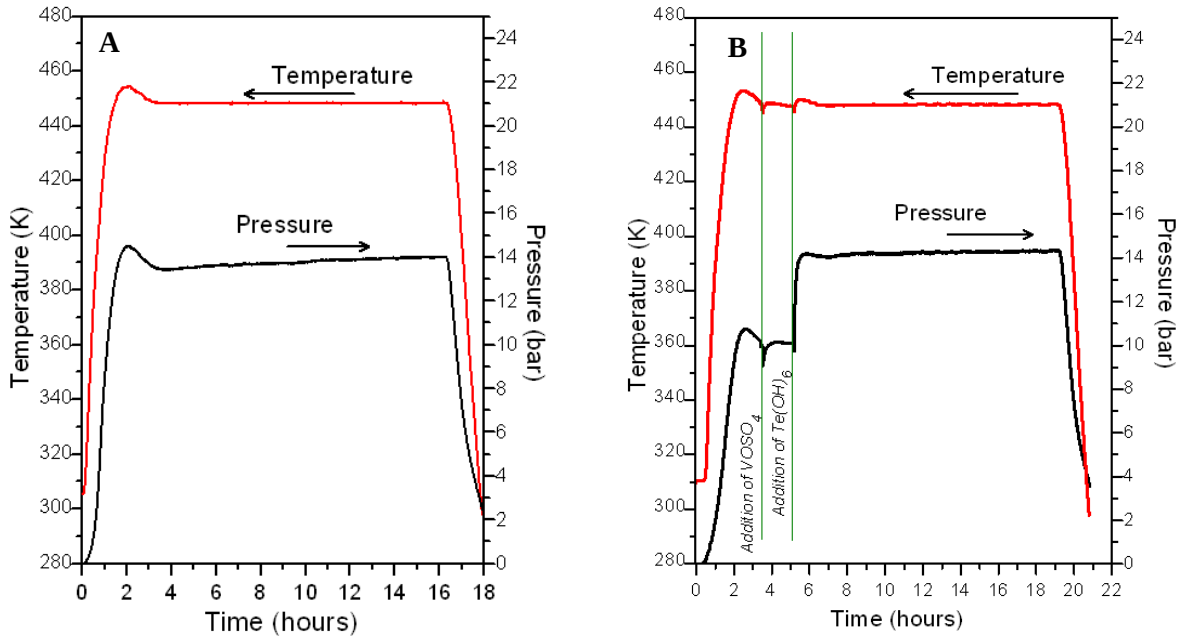

Figure S1. Temperature and pressure profiles during classical hydrothermal synthesis of MoVTeNb oxide over 17 h (A) and step-wise synthesis of the phase-pure M1 precursor (B).

1.2. Step-wise hydrothermal synthesis of MoVTeNb oxide

For the step-wise M1 synthesis, the same amounts of the same reactants as described above were used. A stirring rate of 250 rpm was applied during the entire experiment. The temperature and pressure

profiles are shown in Fig. S1B. The synthesis was performed in the following manner: $(NH_4)_6Mo_7O_{24}$ and $NH_4[NbO(C_2O_4)_2]\cdot 9.7H_2O$ were dissolved subsequently in 170 mL of distilled H_2O in the autoclave at 300 K. The resulting Mo-Nb solution (concentration of Mo of 0.33 mol/L) was heated in the closed autoclave at 5 K/min up to 448 K and then reacted for 1 h 45 min at this temperature. At that point, 30 mL of a solution of $VOSO_4$ containing 16.6 mmol V was pumped at a rate of 20 ml/min using a HPLC Smartline Pump 1000 (Knauer). The Mo+V+Nb mixture was allowed to react for 1 h 45 min at 448 K and then 30 mL of a solution of $Te(OH)_6$ containing 15.3 mmol Te was added at a rate of 20 mL/min. The resultant mixture containing the 4 metals was allowed to react for 14 h at 448 K (autogeneous pressure ca. 14 bar) and then cooled down (1.6 K/min) to room temperature. The suspension obtained after hydrothermal synthesis was separated by centrifugation at 3600 rpm for 10 min. The solid fraction was washed with 100 mL of H_2O and then centrifuged again at 3600 rpm for 30 min. Finally, the solid was dried at 353 K for 16 h to obtain the precursor oxide. Thermal treatment of the precursor was done in a rotary tube furnace (Xerion) under Ar flow (100 ml/min) at 923 K (heating rate 15 K/min) for 2 h resulting in phase-pure M1 (internal sample number 12639) The precursor yield of the step-wise M1 synthesis was 55 wt.% (8.1 g). The synthesis was reproduced two times (internal sample numbers 13014, 13212).

1.3. Characterization techniques

In-situ Raman measurements were done with a Kaiser Optics Raman Spectrometer RXN1 equipped with a fiber-optic probe head for in-situ analysis, resistant to hydrothermal conditions (T_{max}= 723 K ; p_{max}=200 bar) using a Laser wavelength of 785 nm for acquisition of spectra. The sapphire crystal in the tip of the probe is responsible for Raman bands at 432, 451, 578, and 752 cm^{-1}, which were used for normalization of spectra. Phase composition of the crystalline samples was determined by X-ray diffraction performed on a Bruker D8 Advance diffractometer using Cu-$K_{\alpha 1}$ radiation. The diffraction patterns of the activated materials were analyzed with the ‘‘TOPAS’’ software (v.2.1, Bruker AXS). For chemical analysis, the samples were mixed with borate flux and fused under formation of flat molten glass discs, which were analyzed by X-Ray Fluorescence spectroscopy using the spectrometer Pioneer S4 (Bruker). The specific surface area was measured using an Autosorb-6B physisorption analyzer (Quantachrome). Eleven points in the linear range of the nitrogen adsorption isotherm (P/P_0= 0.05–0.3) measured at 77 K were used to calculate the BET surface area. Before adsorption, the samples were degassed at 393 K for 2 h. The M1 catalysts were tested in partial oxidation of propane at temperatures between 633 and 673 K applying a contact time of 1.8 g_{cat}s/ml and a molar ratio of propane/oxygen/water = 1:2:13.333 using nitrogen as balance ($C_3H_8/O_2/H_2O/N_2$ = 3/6/41/50). The catalytic tests were carried out in a setup for selective oxidation (Integrated Lab Solutions, Berlin, Germany) using eight parallel fixed bed quartz reactors at atmospheric pressure. For the measurements, 300 mg of the catalyst was diluted with 2.7 g of silicon carbide (ratio 1:10) for minimization of temperature gradients. Reactants and products were analyzed by online gas chromatography (Agilent 7890) achieving a mass balance of 99.7 %. Separation of the permanent gases CO, CO_2, N_2, and O_2 was performed with a combination of a Plot-Q and a Plot-molsieve column connected to a thermal conductivity detector (TCD). Propane, propylene, acetic acid and acrylic acid were separated using a combination of a Plot-Q and a FFAP column connected to a flame ionization detector (FID).

2. Chemical analysis of hydrothermal reaction intermediates

In order to elucidate the time dependence of the classical hydrothermal reaction,[1] the synthesis was carried out according to the procedure described in section 1.1 of the Supporting Information for 1, 2, 12, 24, and 48 h. After hydrothermal reaction, the resulting slurry was separated by centrifugation into the mother liquor and the solid fraction. Chemical analysis of the solid and the liquid fractions (Fig. S2) shows that niobium is almost completely precipitated, while a considerable amount of Mo, V, and Te remains in the liquid phase. With increasing reaction time, vanadium is progressively incorporated into the precipitate at the expense of molybdenum and, to a lesser extent, of tellurium.

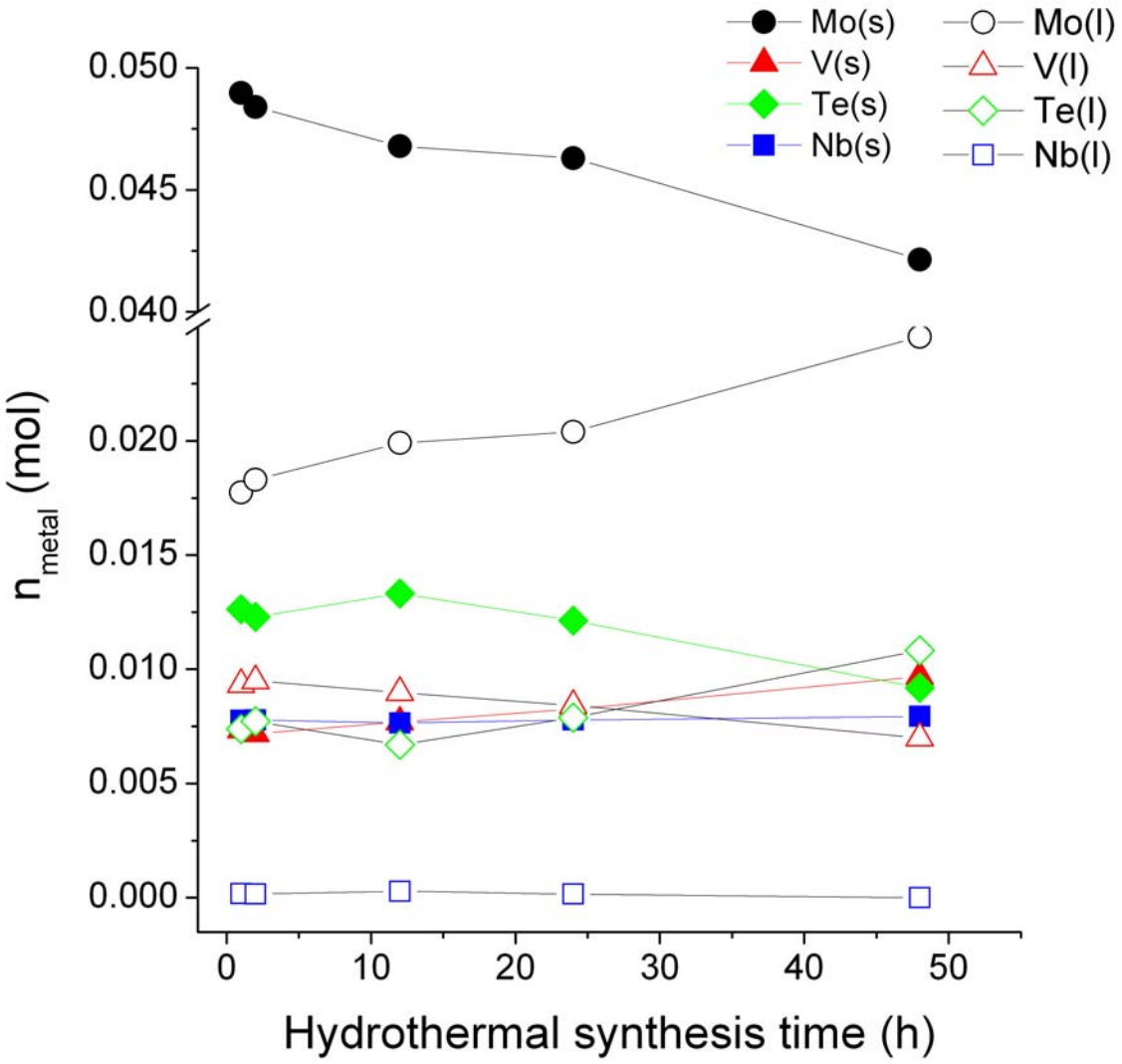

Figure S2. Chemical composition of liquid (open symbols) and solid (filled symbols) fractions separated after hydrothermal synthesis with increasing time. The data points correspond to the final products shown in Figure 1.

3. Assignment of Raman bands observed during classical hydrothermal synthesis of MoVTeNb oxides

3.1. Preparation of the aqueous suspension before hydrothermal synthesis

All bands observed are mentioned in the text even if the spectra are not shown in the entire range. Figure 2 in the main text shows the Raman spectra taken during preparation of the initial synthesis gel at 313-353 K. The typical spectrum of an aqueous solution of ammonium heptamolybdate (pH=5.1, T=313 K) with bands at 940 and 894 cm^{-1} due to Mo-O stretching vibrations of terminal Mo=O and bridging Mo-O-Mo moieties, respectively, immediately changes upon addition of small amounts of $VOSO_4$. At a V/Mo atomic ratio of 0.05 (pH=4.8), new bands appear at 217(vw), 241, 820, 966, and 982(sh) cm^{-1}, while the band at 894 cm^{-1} completely disappears and the band at 940 cm^{-1} decreases in intensity (Fig. S3, and green line in Fig. 2 in the main text). This indicates the formation of Mo-V heteropolyanions consisting of two octamolybdate units connected by vanadyl groups.[2] Complete addition of $VOSO_4$ until reaching the target V/Mo ratio of 0.25 results in an acidification of the

medium (pH = 2.5). Bands at 945 (m), and at 868 (s) cm^{-1} with a shoulder at 840 cm^{-1} are developed (Fig. S3, Fig. 2), pointing to the formation of mixed MoV Keplerate anions in solution, since peaks at 941 (w), and 872 (s) cm^{-1} have been assigned to the M=O stretching vibration and the A_{1g} breathing mode, respectively, of spherical $\{Mo_{72}V_{30}\}$ Keplerate species.[3] The broad appearance between 1000 and 940 cm^{-1} may indicate the additional contribution of macroisopolyanions $[Mo_{36}O_{112}]^{8-}$, which display Raman bands at 982, 953, and 904 cm^{-1} in aqueous solution.[4] For reference, a solution of ammonium heptamolybdate containing Mo in a concentration of 0.133 mol/l (assuming that all vanadium in the MoV solution is incorporated into a $\{Mo_{72}V_{30}\}$ Keplerate species) was acidified by addition of 2 M HNO_3. At pH=3.3 and lower, the spectrum is dominated by bands at 981, 954, and 900 cm^{-1} due to $[Mo_{36}O_{112}]^{8-}$. The spectrum at pH=2.2 is shown in Fig. S3.

Addition of $Te(OH)_6$ to the Mo-V solution (final pH=2.1) did not change the Raman bands very much, apart from the small contribution at 644 cm^{-1}, due to telluric acid in solution.[5] The MoVTe solution was then heated up to 353 K, following the recipe previously published.[1b] When temperature achieves values higher than 348 K, a slow reaction is observed. The bands at 945, 868, and 840 cm^{-1} due to the $\{Mo_{72}V_{30}\}$ Keplerate decrease with time while new bands at 967, 808, 786 (sh) and 773 cm^{-1} are growing. The change of Raman bands is coinciding with a change in color from dark red to cappuccino color and finally intense yellow together with the formation of a fine suspension. We suggest that the new Raman bands are due to the stretching vibration of Mo=O terminal, and Mo-O-Mo bridging bonds, respectively, in the heteropolymolybdate $[(TeO_3)_2Mo_{12}O_{36}]^{4-}$ identified by Himeno et al.[6] These authors described the formation of $[(TeO_3)_2Mo_{12}O_{36}]^{4-}$ as a reaction between the macroisopolyanion $[Mo_{36}O_{112}]^{8-}$ and $(TeO_3)^{2-}$ ions in acidic medium. In view of the structural similarities between $\{Mo_{36}\}$ and the $\{Mo_{72}V_{30}\}$ Keplerate,[7] and the absence of any other intermediate in the Raman spectra, it is presumed that a related reaction takes place in the Mo-V solution in presence of $Te(OH)_6$. Due to additional Raman bands, the parallel presence of telluric acid (644 cm^{-1})[5] Anderson-type heteropolyanions $[Te(Mo,V)_6O_{24}]^{n-}$ (950, 1010 cm^{-1})[8], and vanadyl sulfate species (bands at 975 and 1050 cm^{-1}) cannot be excluded. Finally, after cooling down to 313 K, the addition of $NH_4[NbO(C_2O_4)_2]\cdot xH_2O$ to the Mo-V-Te solution at T=313 K (final pH=1.6) did not produce any further change in the Raman spectrum.

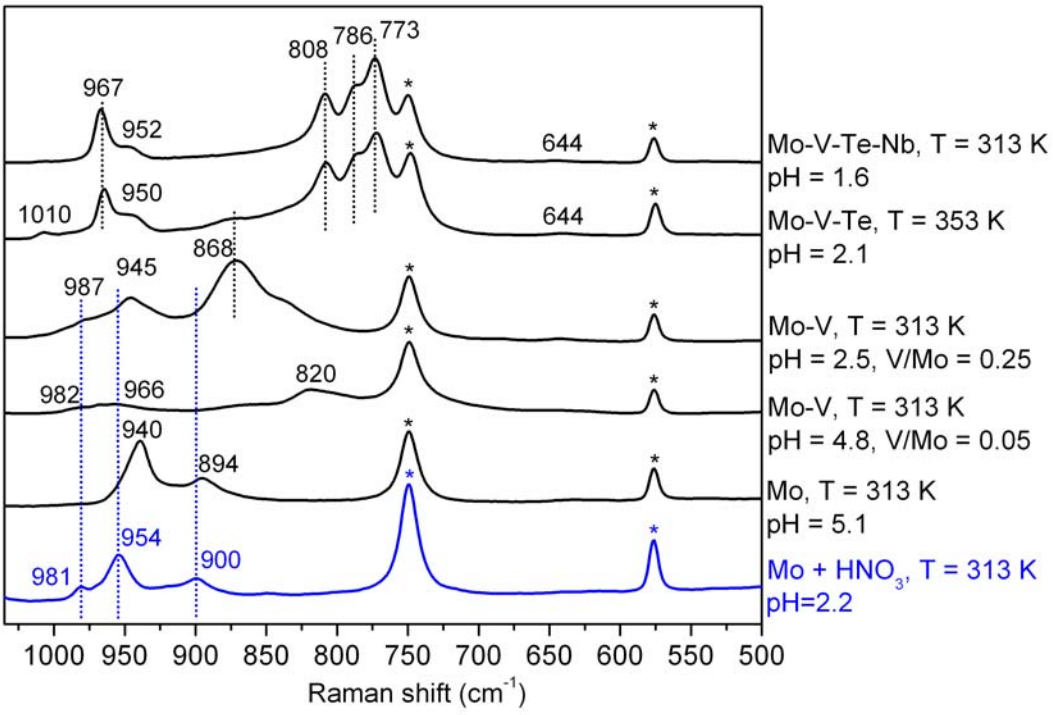

Figure S3. Selected *in-situ* Raman spectra showing the main intermediates during preparation of the aqueous suspension before hydrothermal synthesis. The spectra correspond to the three-dimensional Figure 2 in the main text. The blue spectrum was obtained by acidification of an ammonium heptamolybdate solution, for details see text. Symbol (*) indicates a band of the sapphire window of the Raman probe.

3.2. Heating from 313 K to 448 K

Figure 3 in the main text shows the Raman spectra taken in the closed autoclave when heating the suspension with a rate of 5 K/min from 313 K to hydrothermal reaction temperature 448 K approaching a pressure of 14 bar (Figure S1A). The intensity of bands assigned to $[(TeO_3)_2Mo_{12}O_{36}]^{4-}$ (967, 808, 786 and 773 cm^{-1}), and $[Te(Mo,V)_6O_{24}]^{n-}$ (1010, 950 and 367 cm^{-1}) decreases rapidly when the temperature exceeds 393 K and bands due to intermediate formation of the decomposition product $[Mo_{36}O_{112}]^{8-}$ are observed at 988, 952 and 912 cm^{-1}. After complete decomposition of the molybdotellurates at 418 K, a new set of broad bands arises in the region associated to M-O-M and Mo=O stretching vibrations at 835 and 930 cm^{-1}, respectively (see also Fig. S4). These bands have been attributed to nano-crystalline M_5O_{14} (M=Mo,V,Nb) oxide by Mestl et al.[9]. The broadness of the band at 835 cm^{-1} can be explained by the heterogeneity of the oxide being formed, with multiple M-O-M bonds. The appearance of nano-crystalline M_5O_{14} in the first moments of the hydrothermal reaction is in good agreement with the predominance of this phase in the product obtained after short hydrothermal reaction times (Fig. 1 in main text). Since Nb is almost completely incorporated into the solid (Fig. S2), it is assumed that this element plays an important role in the formation of the nano-crystalline M_5O_{14} owing to its preference to occupy the MO_7 pentagonal bypiramidal position in the $\{(M_5)M\}$ units.[10]

3.3. Hydrothermal reaction at 448 K

Only moderate changes of the Raman spectra have been observed within the 15 hours that the synthesis was monitored under isothermal conditions at T=448 K and p=14 bar (Fig. S4). During the first 2-3 hours, the intensity of the bands at 835 and 980 cm^{-1} decreases slightly, while a broad and ill-defined signal in the 600-1000 cm^{-1} region arises. After 1 hour, a shoulder at 800 cm^{-1} is visible, and another at 875-880 cm^{-1} appears ca. 2 hours later. Together with these changes, a band appears at 325 cm^{-1}. The band at 952 cm^{-1} remained in all the spectra indicating that $\{Mo_{36}\}$ anions are found in solution during the whole process. The spectral changes become more evident by analyzing the covariance of the bands during the 14 hours of isothermal period (Fig. 4 in the main text). The analysis shows that the contributions at 835 cm^{-1} and 952 cm^{-1} remained unchanged during the entire reaction. This observation supports the assignment of these bands to vibrations in the $\{(M)M_5\}$ units of the precipitated phases M_5O_{14} and M1, and to $[Mo_{36}O_{112}]^{8-}$ anions in solution, respectively. The macro-isopolyanions $\{Mo_{36}\}$ can be considered as a species existing in equilibrium with the solid phase, being responsible for the substantial amount of Mo detected in solution after synthesis. The main changes are related to the growth of bands at 969, 931, 880, 800, 726, and 323 cm^{-1}. Since the resulting product is the precursor of a mixture of M1, M2, M_5O_{14} and MO_2 phases (Fig. 1), an unambiguous assignment of these bands is not possible. The spectral patterns are in good agreement with Raman measurements of M1 and M2 phase mixtures published in the literature.[11]

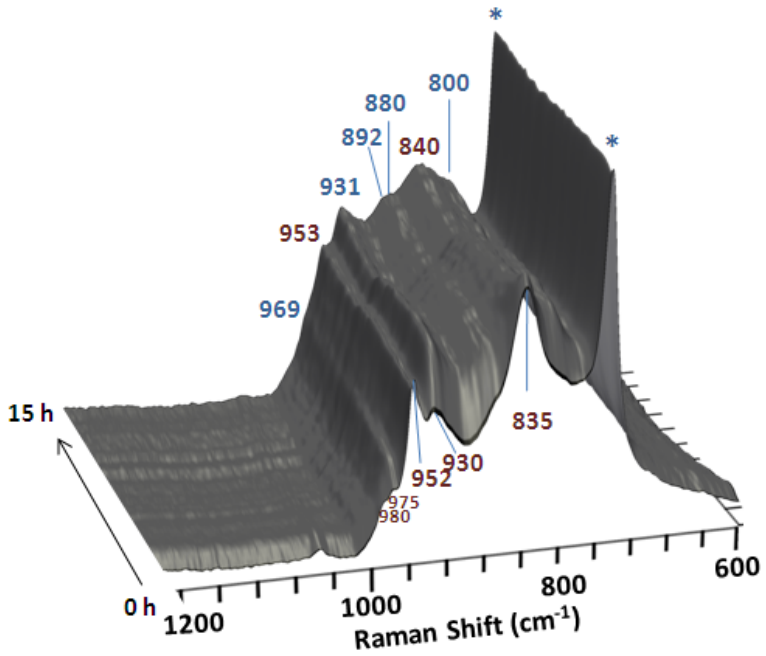

Figure S4. Raman spectra taken during 15 hours in the isothermal stage of hydrothermal synthesis of MoVTeNb oxide (448 K, ca. 14 bar); (*) symbols indicate a band of the sapphire window of the Raman probe.

4. Assignment of Raman bands observed during step-wise hydrothermal synthesis of nano-crystalline M1

The step-wise synthesis of nano-crystalline M1 described in Section 1.2 of the Supporting Information (Fig. S1B) was also monitored using *in-situ* Raman spectroscopy. In the following, the spectroscopic changes happening during the individual steps are described and interpreted. All bands observed are mentioned in the text even if the spectra are not shown in the entire range.

4.1. Reaction of molybdenum and niobium precursors

At first, an aqueous solution of ammonium heptamolybdate and niobium oxalate containing the metals in a Nb/Mo molar ratio of 0.12 was allowed to form nano-crystalline M_5O_{14} at 448 K and 9.5-10 bar (autogeneous pressure) for 1 hour and 45 minutes (Fig. S1B). The *in-situ* Raman spectra measured after mixing of the two components are characterized by bands at 951 and 904 cm^{-1} due to ammonium heptamolybdate and monomeric molybdodioxalate,[12] respectively (Fig. S5). At 448 K, these bands disappear and a new band at 930 cm^{-1} dominates, which indicates that the degree of polymerization increases[12] and $\{Mo_{36-x}Nb_xO_{112}\}$ anions are present in solution. After holding the temperature for 1 hour and 45 min at 448 K, precipitation of a nanocrystalline oxide containing $\{(M)M_5\}$ units is observed, giving rise to a band at 812 cm^{-1}.

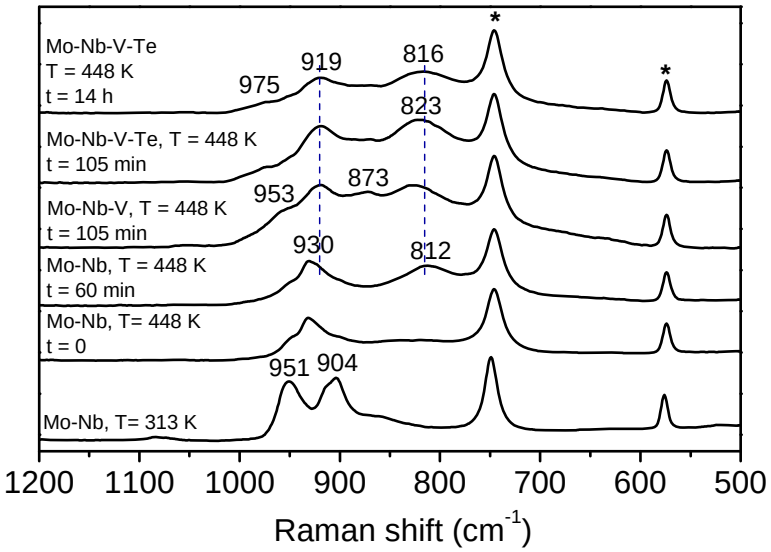

Figure S5. *In-situ* Raman spectra measured during step-wise M1 synthesis. Reaction conditions are indicated in the figure. (*) Symbols indicate bands of the sapphire window of the Raman probe.

4.2. Addition of $VOSO_4$

After the Mo-Nb precursors were reacted for 1 hour and 45 min at 448 K as described in Section 4.1, an aqueous solution of $VOSO_4$ was pumped into the autoclave adjusting the V/Mo ratio to 0.25 (Fig. S1B). The Mo/V/Nb mixture was again allowed to react for 1 hour and 45 minutes at the same temperature with the aim to cross-link the pentagonal units with vanadium species, as depicted in Scheme 1 in the main text. The addition of V generates new bands at 953, 873 and 314 cm^{-1}, and causes a shift of the bands at 930 and 812 cm^{-1} towards 920 and 826 cm^{-1} (Fig. S5). The shift might indicate that Mo units are partially substituted by V atoms in both nanocrystalline M_5O_{14} and the $\{Mo_{36-x}Nb_xO_{112}\}$ anions in solution.

4.3. Addition of $Te(OH)_6$

Finally, an aqueous solution of $Te(OH)_6$ was added achieving a molar ratio Te/Mo = 0.23. The Mo-V-Te-Nb mixture was allowed to react for 14 hours (Fig. S1B). The introduction of Te is responsible for a decrease of the new bands detected after introduction of V, and a slight shift of the two main peaks near 920 and 820 cm^{-1}. These two peaks are characteristic for nano-cystalline M1, because the isolated precipitate can be crystallized at 923 K in argon atmosphere resulting in phase-pure M1 (Fig. S6). The Raman spectra did not change during the last 11 hours of hydrothermal reaction (Fig. S5).

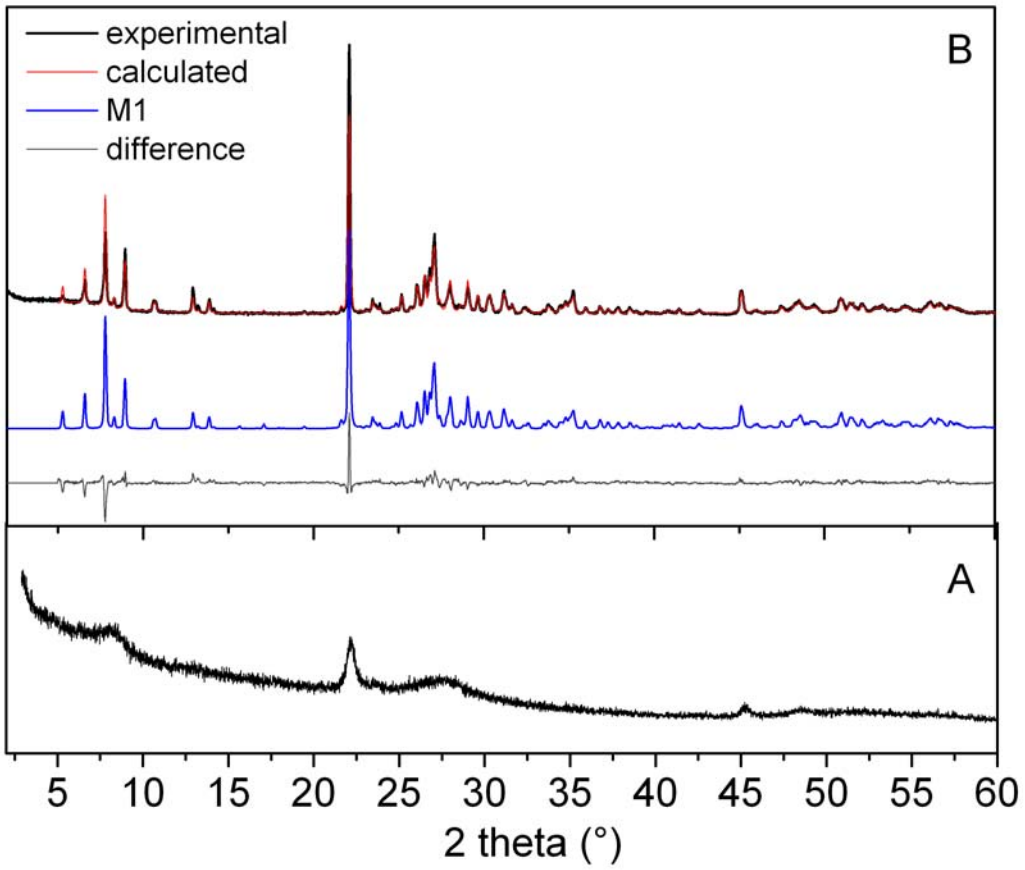

Figure S6. X-ray diffraction patterns of the nano-crystalline product of the step-wise hydrothermal synthesis (A, internal sample ID 12636) and the crystalline, phase-pure M1 catalyst (B, internal sample ID 12639) obtained by crystallization of the precursor in Ar at 923 K.

5. Material properties of the synthesized MoVTeNb oxides

The step-wise synthesis results in a nano-crystalline precursor of the composition $Mo_1V_{0.2}Te_{0.2}Nb_{0.2}O_x$ that is crystallized resulting in phase-pure M1 by annealing in Ar at 923 K (Chapter 1.2 of the Supporting Information). The Raman spectrum of the activated crystalline solid of the step-wise MoVTeNb oxide synthesis is compared with the spectrum of the precursor in Fig. S7 showing striking similarities, but increased intensity of the bands at 872 cm^{-1} and <500 cm^{-1}. The peak at 872 cm^{-1} could be related M-O stretching vibrations in structural components typical for M1, such as octahedra that bridge the hexagonal and heptagonal rings. This tentative assignment is in agreement with the increase of this band after introduction of V, since vanadium preferentially occupies these bridging octahedral sites.[10] The spectrum of the supernatant mother liquor is comparatively poor in features indicating residual vanadyl sulfate, oxalate ions and molybdenum species in solution.

Compared to the classical hydrothermal recipe, the yield of the solid precursor was increased by 10 % applying the novel synthesis procedure (Table S1), which is of advantage also in view of an improved control with respect to the final chemical composition of the solid. A higher synthesis temperature of 463 K is required in the classical synthesis to achieve the synthesis of a precursor of phase-pure M1 in a similar synthesis time. Chemical composition, lattice constants and specific surface area of the two M1 products differ (Table S1). The higher surface area of the new M1 is a consequence of the initial precipitation of Mo species during the mixing and heating stages, that in the new synthesis method takes place through a controlled decomposition of Mo oxalates during the heating process. The

increased Mo content is attributed to the addition of Te in an advanced stage of the synthesis that avoids the formation of Te-Mo polyanions, which usually stay in solution under the given conditions. The differences are reflected in the catalytic performance of the two catalysts in partial oxidation of propane to acrylic acid. The significant increase in activity is not only due to the higher specific surface area of the M1 prepared by step-wise synthesis, but also due to a higher intrinsic activity, while the new catalyst is characterized by distinguished selectivity to acrylic acid resulting in an increase in space time yield by a factor of five.

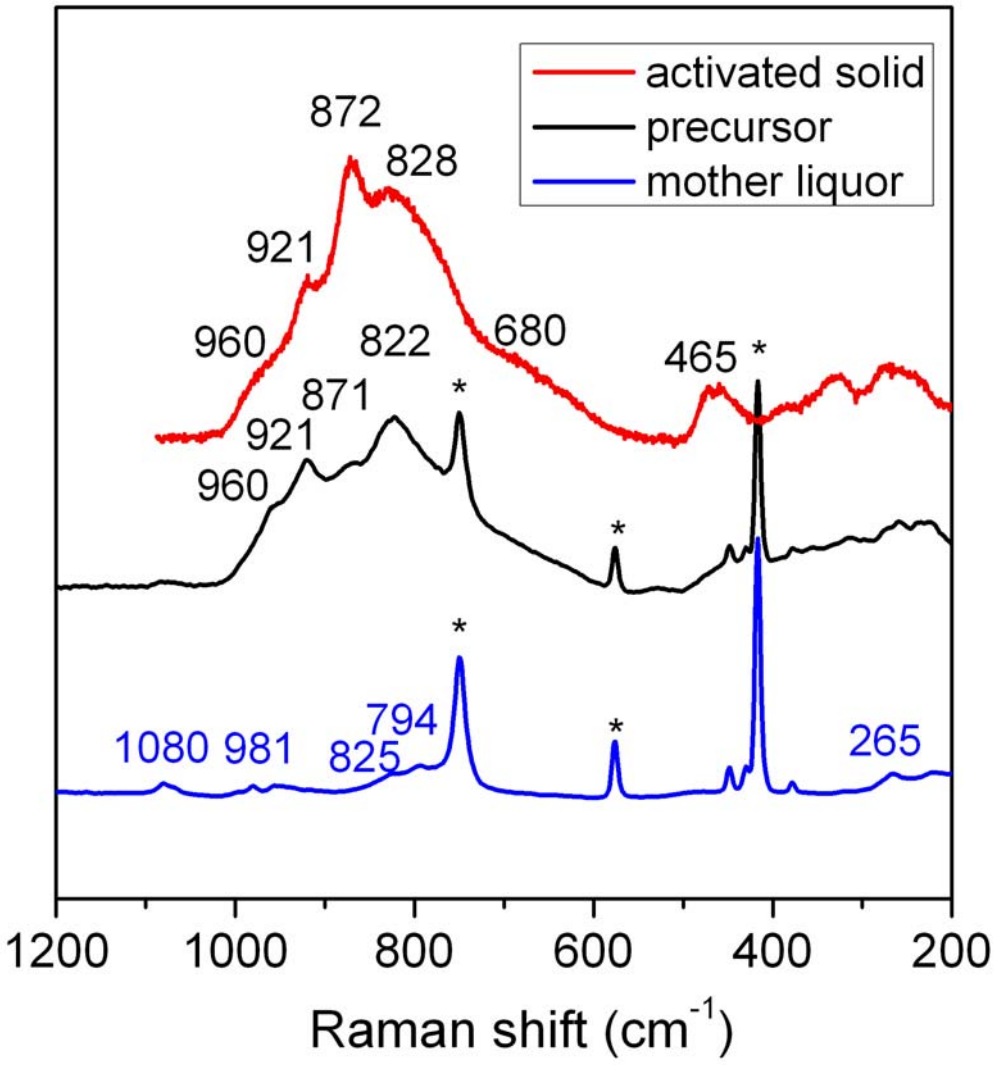

Figure S7. Raman spectra of mother liquor (blue trace), wet solid precursor (black trace), and crystalline M1 (red trace). (*) Symbols indicate bands of the sapphire window of the Raman probe.

Table S1. Characteristics of phase-pure M1 catalysts prepared by the classical and the novel, step-wise method.

	Classical M1 synthesis (catalyst ID 11811)	Novel, step-wise M1 synthesis (catalyst ID 12639)
Hydrothermal conditions	T=463 K Mo/Nb/V/Te for 12 h	T=448 K Mo/Nb for 1.75 h Mo/Nb/V for 1.75 h Mo/Nb/V/Te for 14 h
Yield of M1 precursor[1]	42 wt.% (6.2 g)	55 wt.% (8.1 g)
Formulation normalized to Mo[2]	$MoV_{0.228}Te_{0.267}Nb_{0.318}$	$MoV_{0.207}Te_{0.180}Nb_{0.207}$
SBET (m^2/g)	1.5	4.7
Lattice parameters (Å) a b c	 21.2246 26.7271 4.01086	 21.1773 26.6651 4.01262
Ea[3] [kJ/mol]	72	55
Space time yield [$mg_{aa}/g_{cat}h$] at 673 K	9.3	48.8

[1] calculated based on the simplified assumption that the metals are present in the highest oxidation state
[2] metal content based on chemical analysis by X-ray fluorescence
[3] based on the consumption rate of propane

6. References

[1] a)D. Vitry, Y. Morikawa, J. L. Dubois, W. Ueda, *Topics in Catalysis* **2003**, *23*, 47; b)A. Celaya Sanfiz, T. W. Hansen, F. Girgsdies, O. Timpe, E. Rödel, T. Ressler, A. Trunschke, R. Schlögl, *Topics in Catalysis* **2008**, *50*, 19.

[2] S. Knobl, G. A. Zenkovets, G. N. Kryukova, R. I. Maksimovskaya, T. V. Larina, N. T. Vasenin, V. F. Anufrienko, D. Niemeyer, R. Schlögl, *Physical Chemistry Chemical Physics* **2003**, *5*, 5343.

[3] a)A. Müller, A. M. Todea, J. van Slageren, M. Dressel, H. Bögge, M. Schmidtmann, M. Luban, L. Engelhardt, M. Rusu, *Angewandte Chemie International Edition* **2005**, *44*, 3857; b)C. Schäffer, A. M. Todea, P. Gouzerh, A. Müller, *Chemical Communications* **2012**, *48*.

[4] a)K.-H. Tytko, B. Schönfeld, B. Buss, O. Glemser, *Angewandte Chemie International Edition in English* **1973**, *12*, 330; b)A. Müller, E. Krickemeyer, S. Dillinger, H. Bögge, W. Plass, A. Proust, L. Dloczik, C. Menke, J. Meyer, R. Rohlfing, *Zeitschrift für anorganische und allgemeine Chemie* **1994**, *620*, 599.

[5] J. Gupta, *Nature* **1937**, *140*, 685.

[6] S. Himeno, K.-i. Sano, H. Niiya, Y. Yamazaki, T. Ueda, T. Hori, *Inorganica Chimica Acta* **1998**, *281*, 214.

[7] A. Müller, C. Serain, *Accounts of Chemical Research* **2000**, *33*, 2.

[8] a)I. L. Botto, C. I. Cabello, H. J. Thomas, *Materials Chemistry and Physics* **1997**, *47*, 37; b)Y. Sun, J. Liu, E. Wang, *Inorganica Chimica Acta* **1986**, *117*, 23.

[9] G. Mestl, C. Linsmeier, R. Gottschall, M. Dieterle, J. Find, D. Herein, J. Jäger, Y. Uchida, R. Schlögl, *Journal of Molecular Catalysis A: Chemical* **2000**, *162*, 463.

[10] P. DeSanto, Jr., D. J. Buttrey, R. K. Grasselli, C. G. Lugmair, A. F. Volpe, Jr., B. H. Toby, T. Vogt, *Zeitschrift fuer Kristallographie* **2004**, *219*, 152.

[11] B. Solsona, M. I. Vazquez, F. Ivars, A. Dejoz, P. Concepcion, J. M. Lopez Nieto, *Journal of Catalysis* **2007**, *252*, 271.

[12] K. Y. S. Ng, X. Zhou, E. Gulari, *The Journal of Physical Chemistry* **1985**, *89*, 2477.